Progress In Electromagnetics Research B, Vol. 14, 65–86, 2009

TRUNCATION EFFECT ON PRECURSOR FIELD STRUCTURE OF PULSE PROPAGATION IN DISPERSIVE MEDIA

J. Qi and A. Sihvola

Department of Radio Science and Engineering
Helsinki University of Technology
P. O. Box 3000, 02015 TKK, Espoo, Finland

Abstract—The dynamic evolutions of full Gaussian and particularly the truncated Gaussian pulses in dispersive Lorentz media are studied numerically in detail. The observed qualitative phenomena lead to revised interpretation regarding both Sommerfeld and Brillouin precursors. Neither strict Sommerfeld nor Brillouin precursor is present for the case of an incident full Gaussian pulse for any finite propagation distance. In addition, the Brillouin effect can be separated into a tail and a forerunner depending on the turn-on point of the initial pulse. Moreover, the essence of an artificial precursor is discussed, which deserves caution when handling the high dynamic range problems by numerical algorithm.

1. INTRODUCTION

The propagation of electromagnetic pulses in dispersive Lorentz media was initially analyzed by Sommerfeld [1] and Brillouin [2, 3] in 1914 using the asymptotic method of steepest descent. They showed analytically that when the pulse penetrates deep into Lorentz media, its dynamics settle into two parts: the Sommerfeld precursor, which is composed of high-frequency components and propagates at the velocity of light in vacuum c, and the Brillouin precursor, which is composed of low-frequency components and arrives later after the Sommerfeld one [4]. Later, Oughstun and Sherman, using modern asymptotic techniques, accomplished a seminal quantitative improvement to describe the propagated field together with a more accurate definition of signal velocity in dispersive media [5]. Based on

Corresponding author: J. Qi (qi.jiaran@tkk.fi).

this approach, the precursor fields of various types of incident pulses in dispersive media, including unit-step-function-modulated pulse, delta-function modulated pulse and Gaussian pulse, were studied [6–11]. Moreover, the contribution from medium dispersion and absorption in Brillouin precursor is described in [12] and possible usages of Brillouin precursor are suggested in [12, 13]. Other useful methods analyzing this problem, such as imbedding method, Green function method, and propagator method, can be found in [14–16]. Also, the reflection coefficient for a plane wave obliquely incident on a Lorentz medium half space is determined analytically in [17].

Recently, strongly dispersive materials have attracted much attention in connection to metamaterial research [18] where it is typical to design composites that consist of small resonating inclusions as building blocks. One of the aims is to fabricate artificial materials with negative refractive index. Such a property can be achieved only within a certain frequency range, and consequently the material parameter properties are strongly dependent on frequency. This leads to further difficulties in the interpretation of the various wave velocities in the medium [19–23] since not only the magnitude of the velocity but also its direction in negative-phasevelocity materials is to be decided. There is clearly a need for further understanding of pulse behavior in complex materials.

The objective in the present paper is to point out that even if the dynamics of the pulse propagation in Lorentz-dispersive media is well studied, the character of the precursor structure calls for additional analysis and interpretation. The focus in the following is to demonstrate that for an incident ideal full Gaussian pulse, there will be neither Sommerfeld nor Brillouin precursor for any finite propagation distance into Lorentz media. However, their appearance depends on whether the Gaussian pulse has a clearly defined turn-on time. In order to achieve these goals, pulse behavior is examined by applying Fast Fourier Transform (FFT) to various Gaussian pulse forms. The full Gaussian pulse is first analyzed, and the results are compared with earlier literature. Then attention is given to the effect of an onset of the pulse. One of the original contributions of the present paper is the analysis of truncated Gaussian pulses (meaning that the Gaussian pulse is multiplied by a Heaviside unit step function and therefore vanishes before a certain zero-crossing point) as incident waves, compared with the full Gaussian pulse case. Finally, the nature of new qualitative observation — artificial precursor — is examined which is relevant in the interpretation of pulse propagation analyses, especially when the spectra are calculated numerically.

2. PROPAGATION OF FULL GAUSSIAN PULSE IN LORENTZ MEDIA

Consider an incident Gaussian-modulated cosine pulse with carrier frequency ω_c and initial pulse width $2\,T$, given by

$$f(t) = e^{-(t/T)^2} \cos(\omega_c t) \tag{1}$$

which is propagating through isotropic non-magnetic material. The spectrum of the incident field given by Eq. (1) could be analytically calculated by Fourier Transform and is expressed as

$$F(\omega) = \frac{T\sqrt{\pi}}{2}\left(\exp\left(-\frac{T^2}{4}(\omega+\omega_c)^2\right) + \exp\left(-\frac{T^2}{4}(\omega-\omega_c)^2\right)\right) \tag{2}$$

The dielectric behavior of the medium is assumed to follow a Lorentz model where the relative permittivity is described as [24]

$$\varepsilon(\omega) = 1 - \frac{b^2}{\omega^2 - \omega_0^2 + 2i\delta\omega} \tag{3}$$

where ω_0 is the resonant frequency, b is the plasma frequency and δ is the damping frequency. The Lorentz model described in (3) is often used in the analysis of artificial dielectrics, artificial magnetic and metamaterials where individual resonating elements are embedded into a background matrix to enhance the dielectric response of the composite [25, 26].

Although the evolution of ultrashort full Gaussian pulse in Lorentz media has been studied thoroughly (see, for example [9–11]), the dynamics of the pulse evolution is very interesting and deserves to be reviewed here. Let us explore the case when the carrier frequency $\omega_c = 5.75 \times 10^{16}\,\mathrm{s}^{-1}$ is near the upper limit of the absorption band $([(\omega_0^2-\delta^2)^{\frac{1}{2}}, (\omega_0^2+b^2-\delta^2)^{\frac{1}{2}}])$ of a Lorentz medium with parameters $\omega_0 = 4\times10^{16}\,\mathrm{s}^{-1}$, $b^2 = 20\times10^{32}\,\mathrm{s}^{-2}$, and $\delta = 0.28\times10^{16}\,\mathrm{s}^{-1}$, and the initial pulse width $2\,T = 0.4\,\mathrm{fs}$. Except T, all the parameters are the same as those in [9–11]. Although a more smoothly varying envelope is chosen, the pulse is still ultrawideband since the $-3\,\mathrm{dB}$ fractional bandwidth is 20.47%, and also note that $T < 1/\delta$. The reason for choosing a broader pulse width than in these references is that, as shown in Fig. 1, the whole spectrum in this case remains practically limited around the carrier frequency and is located within the most dispersive region. This leads to the fact that the pulse decays much more strongly than in the results shown in [9, 10], which reveals interesting features and provides better understanding concerning Sommerfeld and Brillouin precursors

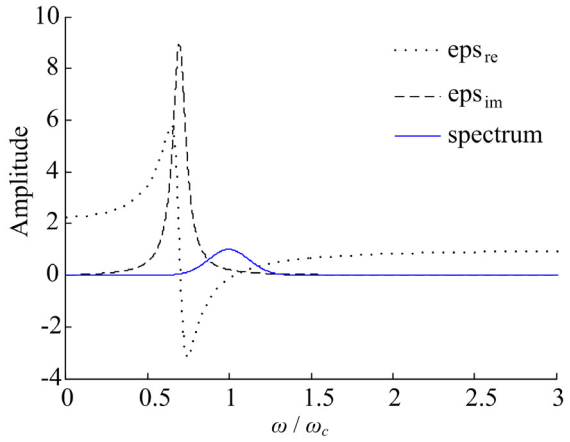

Figure 1. The spectrum of full Gaussian pulse used in the analysis (solid curve) and complex permittivity of the selected Lorentz medium (dotted and dashed curves). The frequency scale is normalized to the carrier frequency ω_c.

in the weak-field regime. In addition, the effect of pulse width is also discussed.

In this paper, FFT is applied to evaluate the transient field at any given propagation distance. In frequency domain approach, an arbitrary plane wave propagates with a phase dependence $\exp(-jkz)$, where $k^2 = \omega^2\mu\varepsilon$. There, at first the spectrum $F(\omega)$ of the initial temporal signal $f(t)$ is calculated by Fourier Transform, then in frequency domain, the propagated spectrum is described as $F(\omega)\exp(-jkz)$, and finally the propagated temporal waveform is computed using Inverse Fourier Transform. Here the FFT and Inverse Fast Fourier Transform (IFFT) algorithms are applied to approximate the Fourier and Inverse Fourier integrals. It should also be noticed that all the results are calculated with identical sample points $N = 10^6$ and computational domain from $-200\,T$ to $200\,T$, which is sufficiently large to model the pulse in Eq. (1). In order to examine the validity of the FFT routine, the spectra are also calculated analytically (by multiplying $\exp(-jkz)$ with the analytical spectrum in (2)) in comparison with the numerical spectra obtained by FFT.

2.1. Dynamic Evolution of Full Gaussian Pulse

The pulse evolution, shown in detail in Fig. 2 as function of the space-time parameter $\theta = ct/z$, can be summarized qualitatively in the following way. When the initial Gaussian pulse propagates inside the

Lorentz medium, its envelope starts to spread out gradually and decay dramatically. In time domain, the pulse oscillations become faster. This is consistent with the developments in frequency domain, where the lower frequency components decay faster than the higher ones. With the increase of propagation distance up to $z = 167.84\, z_d = 2\,\mu\text{m}$, where z_d ($= 11.92\,\text{nm}$) denotes the e^{-1} absorption depth at the carrier frequency ω_c [11], a much lower frequency tail (in both time and frequency domains) is witnessed just after the initial signal. This tail attenuates much more slowly than the initial Gaussian pulse. As the pulse continues to propagate, a very-quick-oscillating structure appears in front of the initial Gaussian pulse, which is very small in amplitude. Further examination shows that it always travels at the light velocity in vacuum c and its amplitude remains nearly invariable (10^{-13}). Let us call this high-frequency structure 'artificial precursor' and the low-frequency tail 'Brillouin tail'. When $z = 251.76\, zd = 3\,\mu\text{m}$, the pulse has developed into clearly three parts: artificial precursor, the initial pulse and Brillouin tail. Finally, the initial Gaussian pulse vanishes leaving only the artificial precursor and Brillouin tail in Fig. 2(e), and again the artificial precursor seems not to decay during propagation. In frequency domain, the comparison between analytical and numerical spectrum in Fig. 2(f) indicates that the artificial precursor deserves further examination.

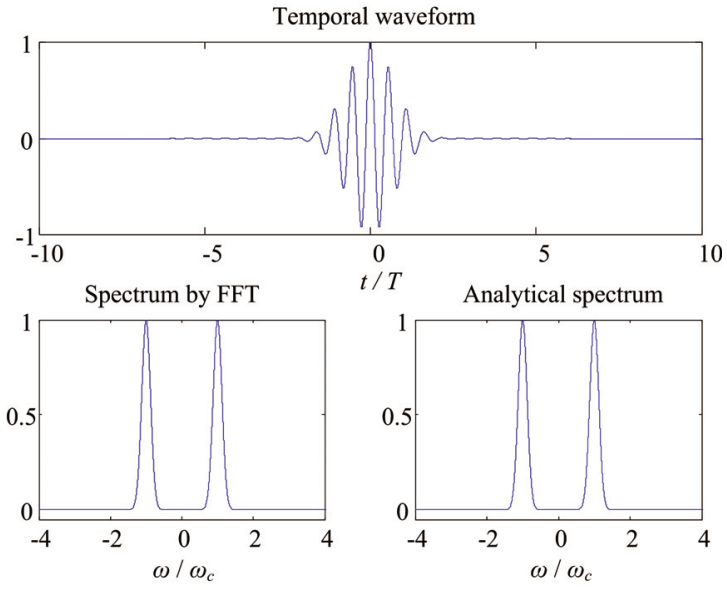

(a) 0 m

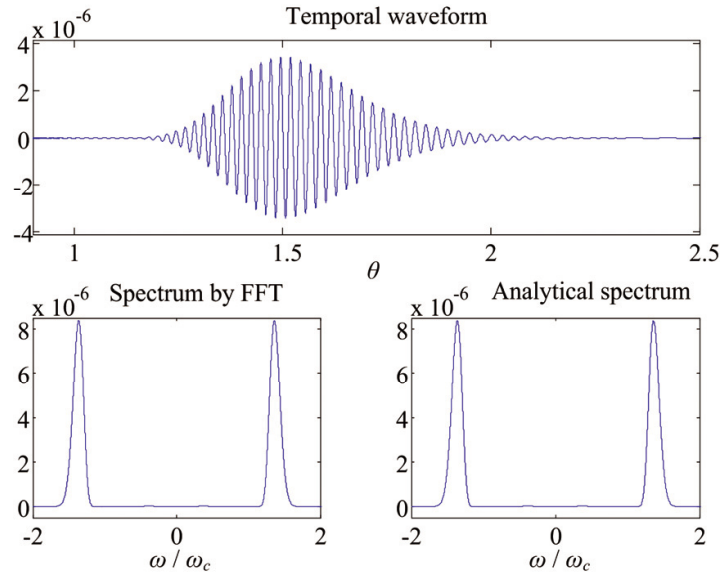

(b) $z = 83.92\ z_d = 1\ \mu\text{m}$

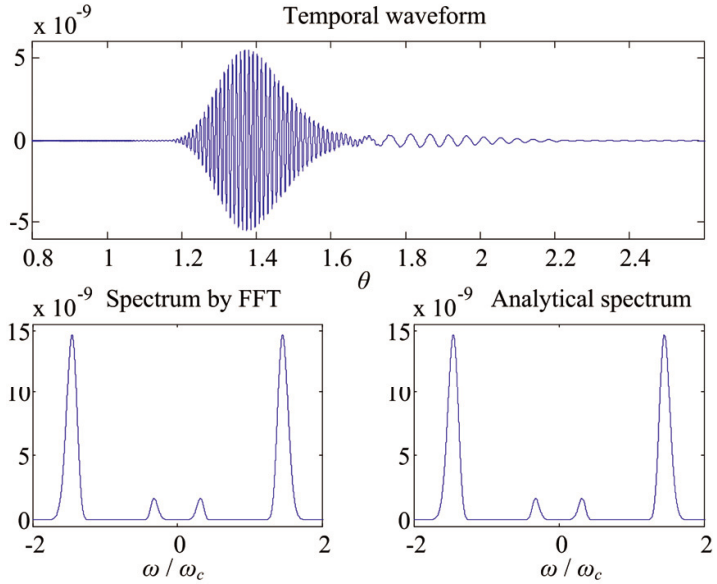

(c) $z = 167.84\ z_d = 2\ \mu\text{m}$

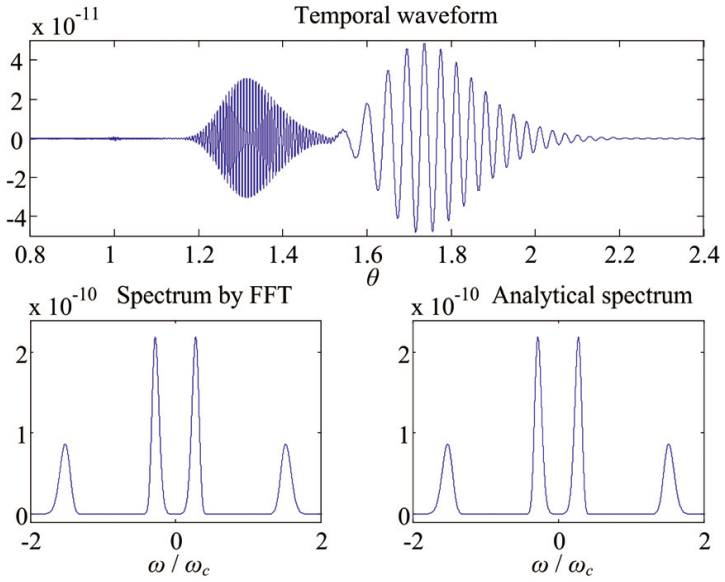

(d) $z = 251.76\ z_d = 3\ \mu\text{m}$

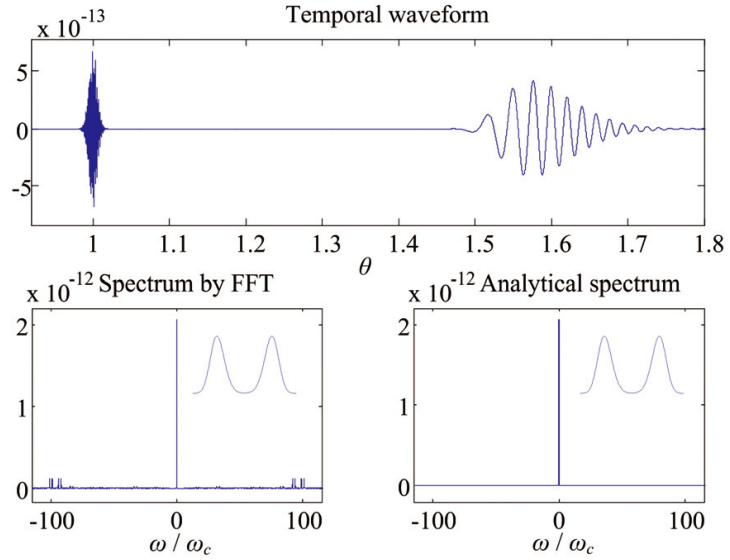

(e) $z = 671.35\ z_d = 8\ \mu\text{m}$

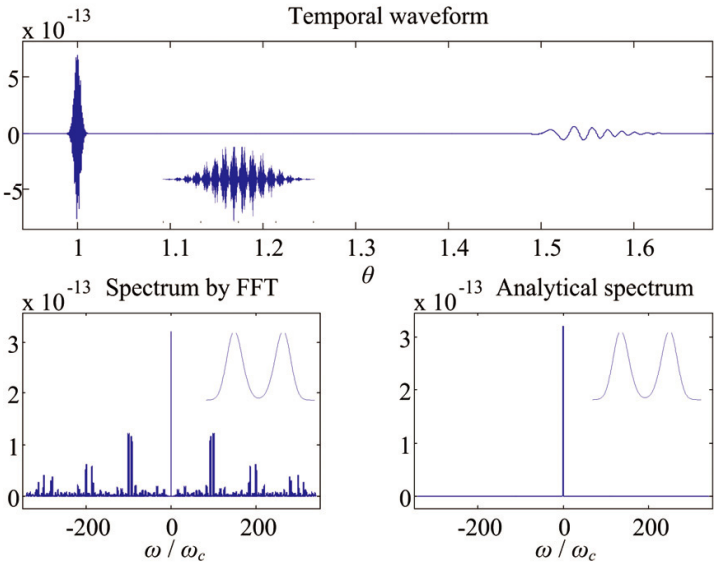

(f) $z = 1090.9\ z_d = 13\ \mu\text{m}$

Figure 2. Dynamic evolution of full Gaussian pulse in Lorentz medium, with absorption depth $z_d = 11.92\,\text{nm}$, carrier frequency $\omega_c = 5.75 \times 10^{16}\,\text{s}^{-1}$, initial pulse width $2T = 0.4\,\text{fs}$.

2.2. Interpretation of the Evolution: Artificial Precursor and Brillouin Tail

It is illustrative to compare the results in Fig. 2 with the results in earlier literature [9]. A similar dynamic evolution is observed despite the different initial pulse width T. However, one major difference is that the pulse in Fig. 2 suffers from a much greater attenuation because the spectrum is more concentrated on the carrier frequency and is located in the most dispersive and attenuation region. Another important distinction lies in the emergence of artificial precursor, whose amplitude (of the order of 10^{-13}) is invariable and comparable with those of initial pulse and Brillouin tail. Great caution should be paid when trying to explain this artifact. Its appearance and velocity (always the vacuum light speed considering the envelope) are not affected much by increasing sample points or computational range.

The proper interpretation of this phenomenon is as follows. In numerical computation, floating-point numbers with only finite digits cannot faithfully mimic the real numbers, which means a non-absolute-zero value could be treated as zero when it is beyond the description

capability of the floating-point numbers with only finite digits. As a result, the full Gaussian pulse can never be achieved numerically, and moreover, despite a large computational domain defined ($[-200\,T$, $200\,T]$ in this paper), the ideal Gaussian pulse is already numerically truncated at a certain fixed position due to finite digits effect of floating-point numbers. This results in the rapidly oscillating artificial precursor. For instance, when the floating-point numbers have 16 digits, the computation accuracy limit (10^{-16}) has already been reached if $t = 6\,T$, where the value of $|f(t)|$ in (1) is approximately 2.6×10^{-16}. That also explains why the computational range, if it is large enough, has basically no effect on artificial precursor. The fact that the origin of this precursor is in the numerics can also be shown from Figs. 2(e) and (f) where it is seen that in case of analytically calculated frequency spectrum the precursor vanishes. In short, the artificial precursor can be considered as an unphysical Sommerfeld precursor. That means, for an incident ideal full Gaussian pulse, no Sommerfeld precursor should appear.

In [9], the author concluded that an input Gaussian pulse will evolve into a pair of pulses: the generalized Sommerfeld precursor, propagating just below c, and the generalized Brillouin precursor. Nevertheless, from the analysis above, it is shown that leave alone the artificial precursor, no precursor fields emerge during the whole dynamics. So instead of generalized Sommerfeld and Brillouin precursors, we call them initial Gaussian pulse and Brillouin tail considering the envelope.

Figure 3 shows the amplitude of the envelope peak of the propagating field. There, the most dramatic message is the enormous attenuation of the initial pulse. Fig. 4 displays the velocities of the envelope peaks of the various components of the pulse. An interesting phenomenon is that the Brillouin tail propagates at nearly a constant velocity v_B roughly equal to $c/n\,(\omega = 0)$, which is usually considered as velocity of the Brillouin precursor. That is because this Brillouin-structure field is composed of low frequency components near DC. The reason for the term 'tail' rather than 'precursor' in this paper is that this Brillouin structure clearly evolves behind the initial pulse, as shown in Fig. 2.

Therefore, for an ideal full Gaussian pulse propagating in Lorentz media, there will be, strictly speaking, neither Sommerfeld nor Brillouin precursor. Admittedly the pulse spectrum in the example was rather narrow but nevertheless the same qualitative conclusions would apply to narrower pulses. Because the spectra of ultrashort pulses spread widely over the whole frequency band, and the larger near-DC and high-frequency components will lead to much larger initial pulse

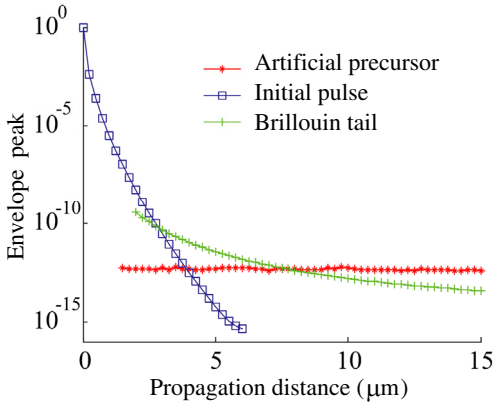

Figure 3. Attenuation of the peak of the pulse envelope of the three different structures of the waveform.

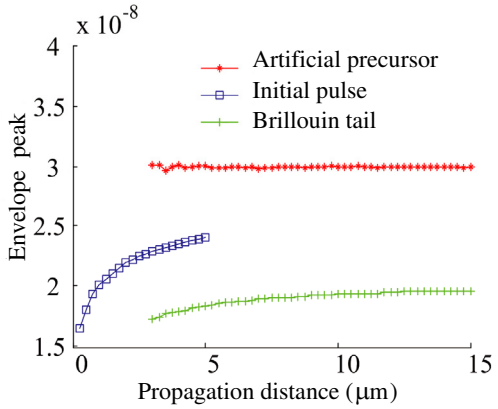

Figure 4. Velocities of the envelope peak of three different structures of the waveform.

and Brillouin tail in amplitude. As a result, the artificial precursor with an invariable amplitude (10^{-13}) becomes invisible but definitely exits.

2.3. Effect of Pulse Width

To further illustrate the point of precursorless evolution of the full Gaussian pulse, let us treat a more wideband pulse. Fig. 5 shows the case where a Gaussian pulse with 10 times narrower pulse width

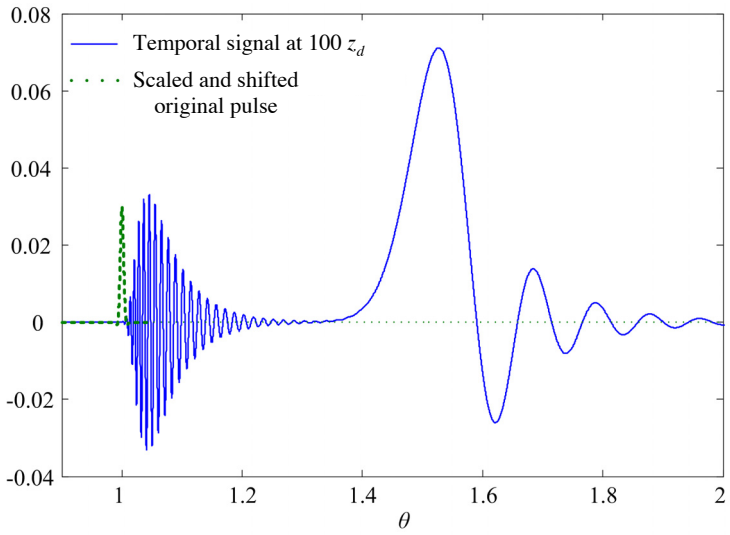

Figure 5. The transient waveform of a ultra-wideband Gaussian pulse with $2T = 0.04\,\text{fs}$ penetrating into the Lorentz medium for $100\,z_d$, together with the dotted curve representing the scaled original pulse which propagates in vacuum for the same distance. The dotted curve, representing the luminally propagating pulse, is clearly ahead of the wake-up of the ultra-wideband full Gaussian pulse.

($2T = 0.04\,\text{fs}$ and $\omega_c = 5.75 \times 10^{16}\,\text{s}^{-1}$) is chosen as the incident field. Fig. 5 shows that although the high-frequency part of the initial pulse travels faster in this case and resembles the Sommerfeld precursor, it is nevertheless subluminal. This can be seen in Fig. 5 by comparison to the position of the initial pulse propagating through free space, whose peak arrives exactly at $\theta = 1$ (here the space-time parameter is defined as $\theta = ct/z$). However, with the continuous decrease of the pulse width, the velocity of the initial pulse will be increasingly approaching the vacuum light speed, and in the limiting case, when the Gaussian pulse evolves into a delta function, the initial pulse could finally be considered as the Sommerfeld precursor.

In order to explore further effect affecting the precursor structure, truncated Gaussian pulses are treated as incident fields in the following section.

3. PROPAGATION OF TRUNCATED GAUSSIAN PULSE IN LORENTZ MEDIA

In order to generate a truncated Gaussian pulse as an input wave, the full Gaussian pulse in Fig. 2(a) is multiplied by a unit-step Heaviside function which triggers at the zero-crossing point of the carrier wave. The zero-crossings are defined by

$$t_0 = \left(k + \frac{1}{2}\right)\frac{\pi}{\omega_c} \tag{4}$$

where $k = 0, \pm 1, \pm 2, \ldots$. In other words, the pulse is silent before this time instant. Different from a full Gaussian pulse, a truncated Gaussian pulse is more realistic with a clearly defined turn-on time at t_0. In order to reveal the truncation effects on pulse dynamics in the mature-dispersion regime, firstly the evolution of a Gaussian pulse truncated at higher order negative zero-crossing point (with negative large k) is analyzed, in which it mimics the full Gaussian pulse and provides a distinguishable comparison. Then, the truncation at lower order negative zero-crossing point is studied to explore the influence of truncation points.

3.1. Comparison between Truncated and Full Gaussian Pulses

Figure 6 illustrates the dynamic evolution of the Gaussian pulse truncated at the negative zero point $t_0 = -0.9\,\text{fs} = -4.5\,T$ when $k = 17$, and the space-time parameter θ is defined as $\theta = (t - t_0)c/z$ (note that $\theta = 1$ corresponds to the luminally propagating signal component). Compared with Fig. 2, the entire dynamic evolution resembles closely that of the previously analyzed full Gaussian pulse. However, a more close comparison in Fig. 7 clearly shows the following: First, a clear-shaped Sommerfeld precursor, traveling exactly at c, arrives as the earliest part of the signal; and second, a clear-shaped Brillouin precursor emerges after the initial pulse but before the Brillouin tail. Also in frequency domain, two new frequency components emerge in Fig. 8(a) besides those in Fig. 8(b). One is the strong DC frequency components corresponding to the Brillouin precursor. The other is the even higher frequency components ranging from $-50\omega_0$ to $50\omega_0$ which corresponds to the Sommerfeld precursor.

This leads to the following significant conclusion: for the full Gaussian pulse case, it is not proper to name the propagated field after precursors, since there is neither strict-speaking Sommerfeld nor Brillouin precursor for any finite propagation distance into the Lorentz

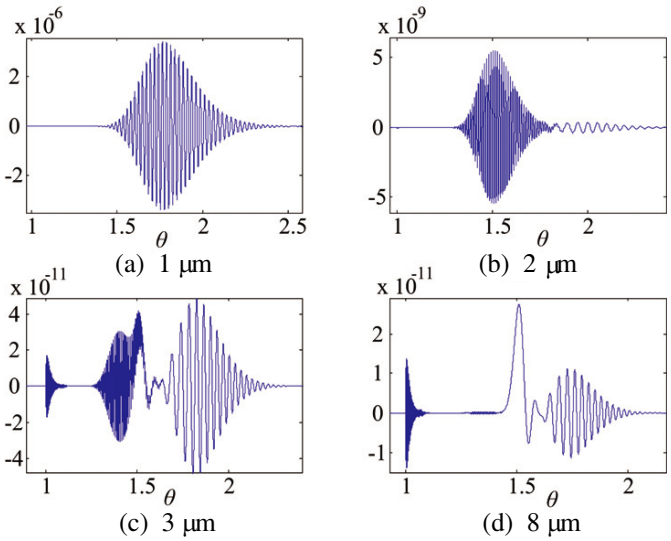

Figure 6. Dynamic evolution of truncated Gaussian pulse at $t_0 = -4.5\,T = 0.9\,\text{fs}$ in Lorentz medium, with absorption depth $z_d = 11.92\,\text{nm}$, carrier frequency $\omega_c = 5.75 \times 10^{16}\,\text{s}^{-1}$, initial pulse width $2\,T = 0.4\,\text{fs}$.

media. Also it clearly shows that the emergence of precursor fields depends on whether the Gaussian pulse has a clearly defined turn-on time.

Next, let us study how a more marked turn-on behavior (a truncation closer to the pulse peak) affects the pulse evolution. The dynamic evolution of the Gaussian pulse truncated at the negative zero-crossing point $t_0 = -0.35\,\text{fs} = -1.8\,T$ when $k = 7$ is illustrated in Fig. 9. Obviously, for the same propagation distance $z = 300\,z_d$, the precursor fields dominate the propagated fields and are much larger in amplitude compared with Figs. 7(a) and 8(a). This evidently shows that the amplitudes of Sommerfeld and Brillouin precursors are chiefly determined by the position of the truncation point; in other words, the derivative of the pulse at the turn-on time has a strong influence on the amplitudes of the precursor fields.

3.2. Truncation Effects on the Sequence of Pulse Components

As already shown in previous section, the turn-on time has a significant influence on the amplitudes of the Sommerfeld and Brillouin precursors

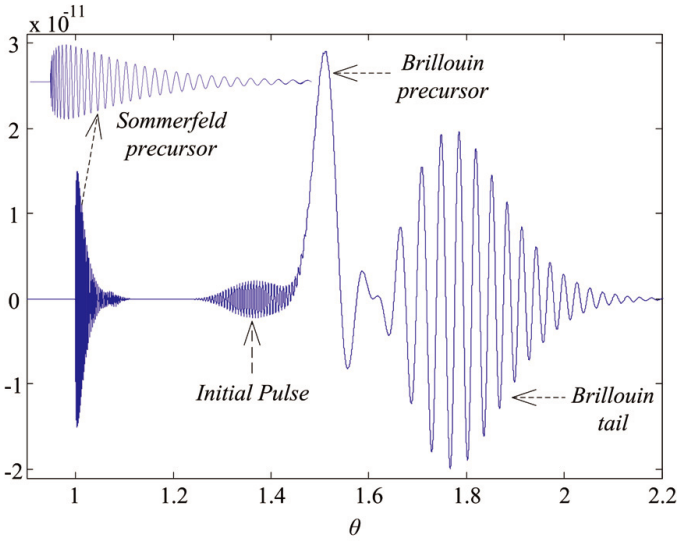

(a) Truncated Gaussian pulses case at $t_0 = -4.5T = 0.9$ fs

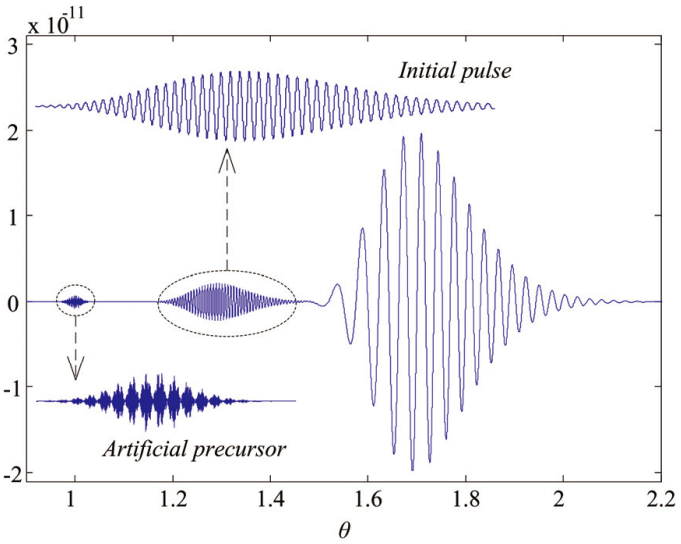

(b) Full Gaussian pulse case

Figure 7. Time-domain comparison between the transient fields of full and truncated Gaussian pulses with the same parameters at $z = 300 z_d = 3.576\,\mu\text{m}$, where absorption depth $z_d = 11.92\,\text{nm}$, carrier frequency $\omega_c = 5.75 \times 10^{16}\,\text{s}^{-1}$, initial pulse width $2T = 0.4\,\text{fs}$.

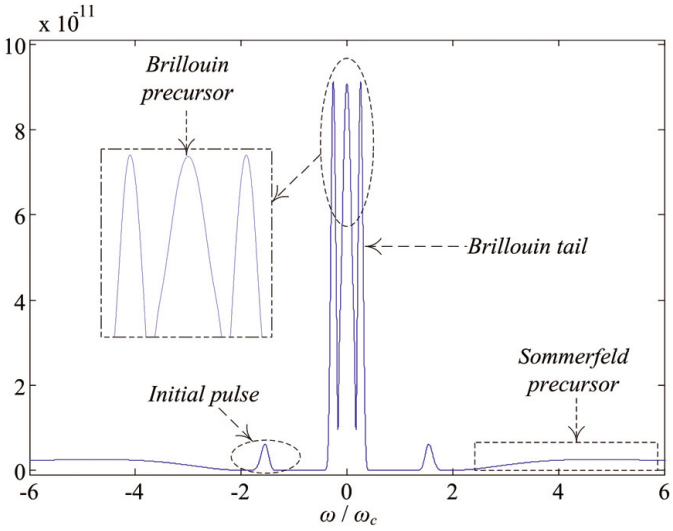

(a) Truncated Gaussian pulses case at $t_0 = -4.5T = 0.9$ fs

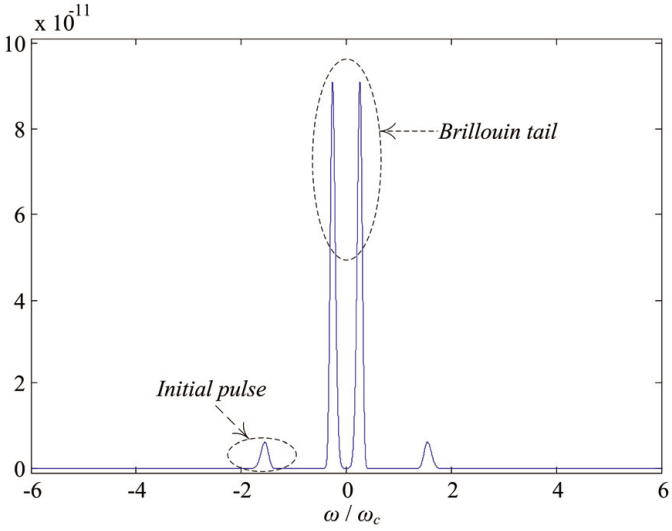

(b) Full Gaussian pulse case

Figure 8. Frequency-domain comparison between the spectra of full and truncated Gaussian pulses with the same parameters at $z = 300z_d = 3.576\,\mu\text{m}$, where absorption depth $z_d = 11.92\,\text{nm}$, carrier frequency $\omega_c = 5.75 \times 10^{16}\,\text{s}^{-1}$, initial pulse width $2\,T = 0.4\,\text{fs}$.

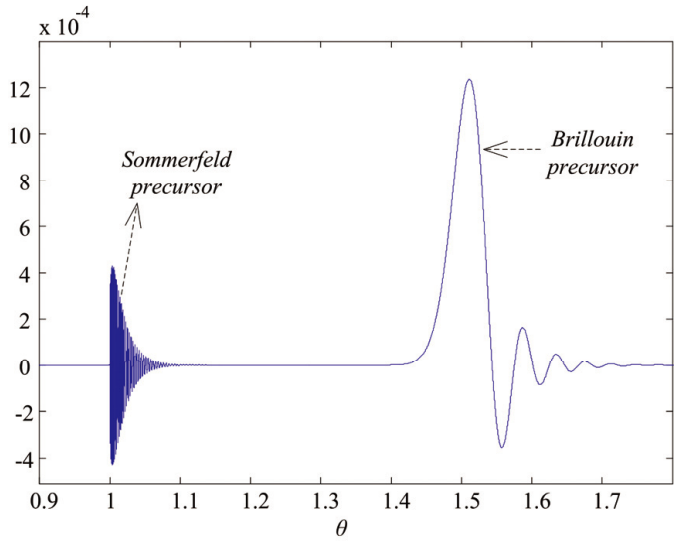

(a) Transient field

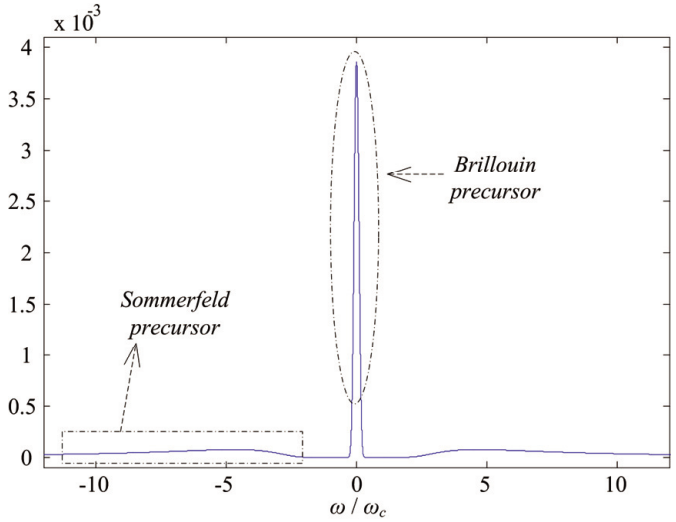

(b) Corresponding spectrum

Figure 9. The transient field of truncated Gaussian pulses with $t_0 = -1.8\,T = -0.35\,\text{fs}$ at $z = 300 z_d = 3.576\,\mu\text{m}$. (Note the 7 orders of larger magnitude of the precursors as compared to Fig. 7(a) and Fig. 8(a), where the truncation is at $t_0 = -4.5\,T = 0.9\,\text{fs}$, and the main pulse is totally overshadowed by the precursors).

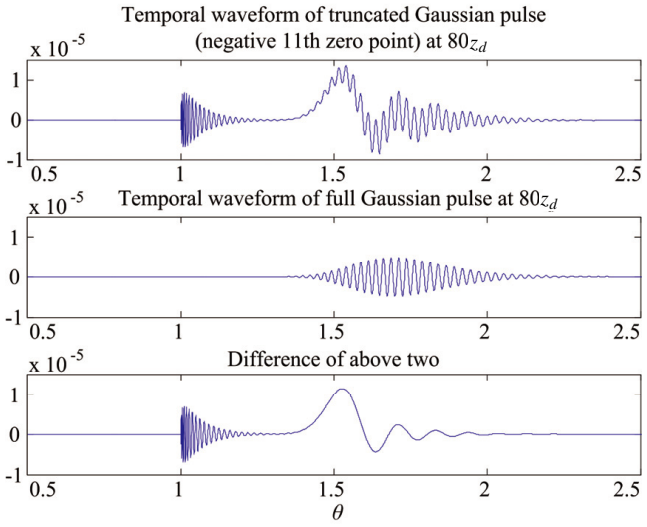

(a) Transient field of truncated Gaussian pulse with t_0 = -2.87 T=-0.574 fs at z = 80z_d = 0.95 μm

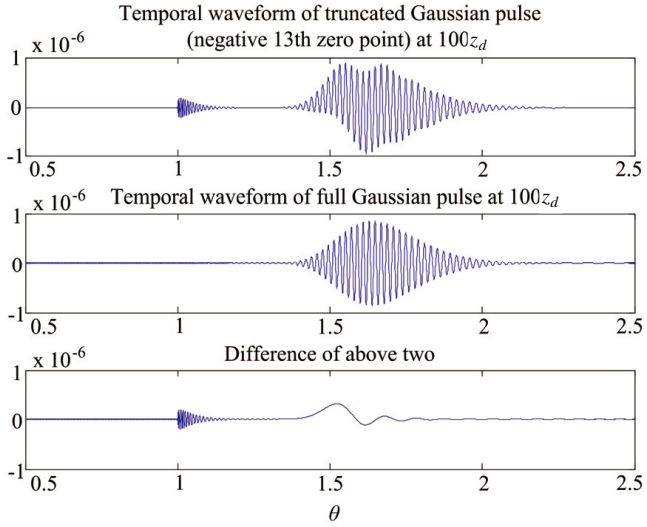

(b) Transient field of truncated Gaussian pulse with t_0=-3.41T=-0.681 fs at z =100z_d=1.19 μm

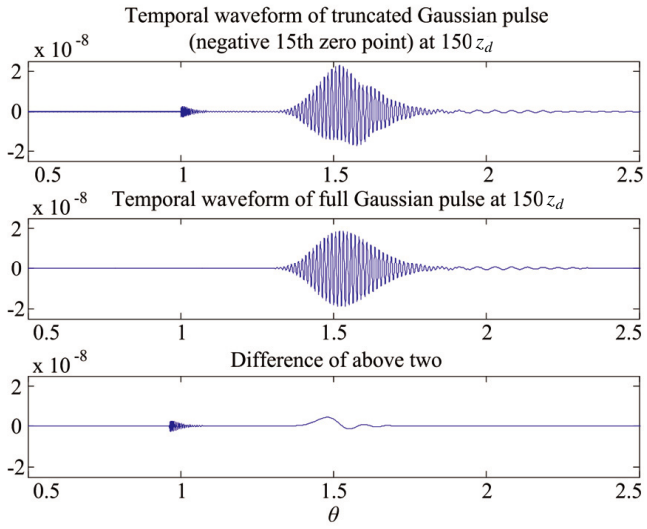

(c) Transient field of truncated Gaussian pulse with $t_0 = -3.96T = -0.792$ fs at $z = 150z_d = 1.79\,\mu$m

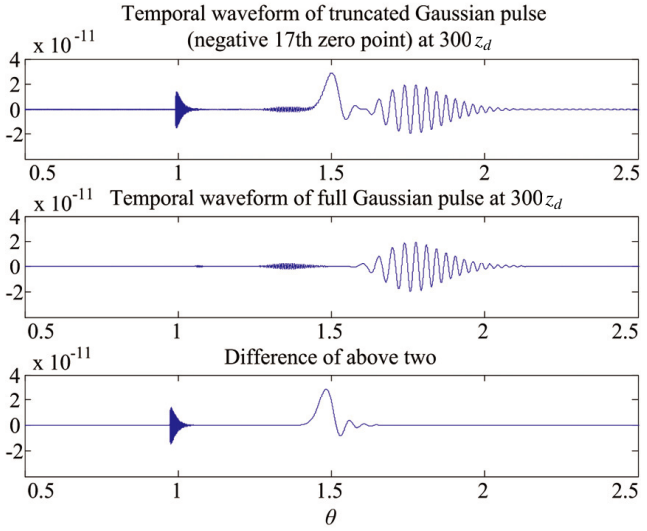

(d) Transient field of truncated Gaussian pulse with $t_0 = -4.50T = -0.901$ fs at $z = 300z_d = 3.57\,\mu$m

Figure 10. The influence of truncation points on the sequence of pulse components.

due to truncation. Also, it should be noticed that for truncated Gaussian pulse with different initial time, the pulse components in the dispersion-mature region may vary greatly not only in amplitude but also in the sequence. In order to qualitatively illustrate this phenomenon, transient fields for different truncated Gaussian pulse in Lorentz medium are computed and compared with those of full Gaussian pulse at the same propagation distance in Fig. 10.

Clearly, the Sommerfeld precursor always arrives firstly and travels exactly at c, while the Brillouin precursor always propagates at the speed of $v = c/n(0) = c/1.5$ and may arrive before, after or overlapping with the original pulse according to varying truncation points. What is more interesting is that the dynamic evolution of truncated Gaussian pulse could actually be interpreted as the combination of the evolution of full Gaussian pulse (the second figure in Fig. 10(a)) and the evolution of the precursor pair due to truncation (the third figure in Fig. 10(a)). As a result, the key distinction of the dynamics lies in the fact that the amplitudes of the precursor pair vary dramatically for different truncation cases. When the truncation introduces a precursor pair small enough, a complete pulse train will be observed as Sommerfeld precursor, main pulse, Brillouin precursor and Brillouin tail shown in Fig. 10(d). Otherwise, when the truncation launches a precursor pair large enough to dominate the evolution, the whole dynamics of full Gaussian pulse will be overlapped and negligible after a certain propagation distance. In all, the Brillouin precursor may appear before, after or overlapping with the main pulse according to different truncation position, and the main pulse and Brillouin tail may be absent while the precursor pair dominate the dynamic evolution.

4. CONCLUSION

The results presented in this paper have shown clearly the role of the truncation on precursor fields when a Gaussian-modulated sinusoidal pulse propagates in dispersive Lorentz media. In the dynamics of a full Gaussian pulse propagation, neither strict Sommerfeld nor Brillouin precursor exists. Rather, the high frequency component should be treated as the initial pulse because of its natural development in the time domain shown in Fig. 2. Furthermore, the low-frequency component should be termed as the Brillouin tail (rather than precursor) since it develops after the main pulse and not in front of it. The studies on truncation cases reveal that the appearances of precursor fields depend on whether the Gaussian pulse has a clearly defined turn-on time and that their amplitudes are chiefly determined by the derivative of the pulse at the turn-on time. The above

statements could also be generalized into other cases when the carrier frequency is not located (as here) in the upper edge of the absorption band. Nevertheless, in such cases similar qualitative phenomena could not be easily observed, because the artificial precursor, the initial pulse, and the Brillouin tail are not comparable with one another in amplitude. When the carrier frequency is above the upper limit of the absorption band ($\omega_c \geq (\omega_0^2 + b^2 - \delta^2)^{\frac{1}{2}}$) where the effective permittivity is close to that of free space as shown in Fig. 1, high-frequency-component structure, referring to so-called initial pulse, resembles the strict Sommerfeld precursor since it dominates the dynamics and travels at velocity very close to c. On the contrary, when the carrier frequency is below the lower limit of the absorption band ($\omega_c \leq (\omega_0^2 - \delta^2)^{\frac{1}{2}}$), the initial pulse could become comparable with the numerical noise (10^{-16}), and the distortion between them will make it difficult to observe the dynamics. This problem can be solved by increasing the digits of floating-point numbers at the expense of more computational time and resources. Anyway, considering the fact that the high frequency structure, either called 'initial pulse' in this paper or 'generalized Sommerfeld precursor' in [9], always travels subluminally, there is still neither strict Sommerfeld nor Brillouin precursor when an arbitrary full Gaussian-modulated cosine pulse propagates in dispersive Lorentz media for a finite propagation distance. However, for the limiting case, when the Gaussian pulse eventually develops into a delta-function-modulated pulse, the 'initial pulse' can be properly considered as the Sommerfeld precursor.

Finally, the discussion about the artificial precursor calls for caution when FFT is used to handle problems with high dynamic range. The appearance of this artifact at the speed of light carries the risk of identifying it with a strict Sommerfeld forerunner. However, due to the fact that a numerical description cannot absolutely reproduce a full Gaussian pulse, the discretization creates an artificial turn-on time which translates into a precursor. This becomes visible when the other physical components of the pulse have decayed to levels below 13 orders of magnitude.

ACKNOWLEDGMENT

This work was supported by the Academy of Finland.

REFERENCES

1. Sommerfeld, A., "Über die fortpflanzung des lichtes in dispergierenden medien," *Ann. Phys.*, Vol. 44, 177–202, 1914.
2. Brillouin, L., "Über die fortpflanzung des licht in dispergierenden medien," *Ann. Phys.*, Vol. 44, 203–240, 1914.
3. Brillouin, L., *Wave Propagation and Group Velocity*, Academic, 1960.
4. Jackson, J. D., *Classical Electrodynamics*, 2nd edition, John Wiley & Sons, Inc., 1975.
5. Oughstun, K. E. and G. C. Sherman, "Propagation of electromagnetic pulses in a linear dispersive medium with absorption (the Lorentz medium)," *J. Opt. Soc. Am. B*, Vol. 5, 817–848, 1988.
6. Wyns, P., D. P. Foty, and K. E. Oughstun, "Numerical analysis of the precursor fields in linear dispersive pulse propagation," *J. Opt. Soc. Am. A*, Vol. 6, 1421–1429, 1989.
7. Oughstun, K. E., P. Wyns, and D. Foty, "Numerical determination of the signal velocity in dispersive pulse propagation," *J. Opt. Soc. Am. A*, Vol. 6, 1430–1440, 1989.
8. Solhaug, J. A., J. J. Stamnes, and K. E. Oughstun, "Diffraction of electromagnetic pulses in a single-resonance Lorentz medium," *Pure Appl. Opt.*, Vol. 7, 1079–1101, 1998.
9. Balictsis, C. M. and K. E. Oughstun, "Uniform asymptotic description of ultrashort Gaussian-pulse propagation in a casual, dispersive dielectric," *Phys. Rev. E*, Vol. 47, 3645–3669, 1993.
10. Oughstun, K. E. and C. M. Balictsis, "Gaussian pulse propagation in a dispersive, absorbing dielectric," *Phys. Rev. Lett.*, Vol. 77, 2210–2213, 1996.
11. Balictsis, C. M. and K. E. Oughstun, "Generalized asymptotic description of the propagated field dynamics in Gaussian pulse propagation in a linear, casually dispersive medium," *Phys. Rev. E*, Vol. 55, 1910–1921, 1997.
12. Ni, X. and R. R. Alfano, "Brillouin precursor propagation in the THz region in Lorentz media," *Optics Express*, Vol. 14, 4188–4194, 2006.
13. Oughstun, K. E., "Dynamical evolution of the Brillouin precursor in Rocard-Powles-Debye model dielectrics," *IEEE Transactions on Antennas and Propagation*, Vol. 53, 1582–1590, 2005.
14. Beezley, R. S. and R. J. Krueger, "An electromagnetic inverse problem for dispersive media," *J. Math. Phys.*, Vol. 26, 317–325,

1985.

15. Kristensson, G., "Direct and inverse scattering problems in dispersive media — Green's functions and invariant imbedding techniques," *Methoden und Verfahren der Mathe-matischen Physik*, Vol. 37, 105–119, 1991.
16. Karlsson, A., "Wave propagators for transient waves in one-dimensional media," *Wave Motion*, Vol. 24, No. 1, 85–99, 1996.
17. Cossmann, S. M. and E. J. Rothwell, "Transient reflection of plane waves from a Lorentz medium half space," *J. of Electromagn. Waves and Appl.*, Vol. 21, 1289–1302, 2007.
18. Sihvola, A., "Metamaterials in electromagnetics," *Metamaterials*, Vol. 1, 2–11, 2007.
19. Bigelow, M. S., N. N. Lepeshkin, H. Shin, and R. W. Boyd, "Propagation of smooth and discontinuous pulses through materials with very large or very small group velocities," *Journal of Physics: Condensed Matter*, Vol. 18, 3117–3126, 2006.
20. Dvorak, S. L. and R. W. Ziolkowski, "Hybrid analytical-numerical approach for modeling transient wave propagation in Lorentz medium," *J. Opt. Soc. Am. A*, Vol. 15, 1241–1254, 1998.
21. Ziolkowski, R. W. and J. B. Judkins, "Propagation characteristics of ultrawide-bandwidth pulsed Gaussian beams," *J. Opt. Soc. Am. A*, Vol. 9, 2021–2030, 1992.
22. Ziolkowski, R. W., "Superluminal transmission of information through an electro-magnetic metamaterial," *Phys. Rev. E*, Vol. 63, 1–13, 2001.
23. Ziolkowski, R. W., "Wave propagation in media having negative permittivity and permeability," *Phys. Rev. E*, Vol. 64, 1–15, 2001.
24. Sihvola, A. H., *Electromagnetic Mixing Formulas and Application*, IEE, 1999.
25. Pendry, J. B., A. J. Holden, D. C. Robbins, and W. J. Stewart, "Magnetism from conductors and enhanced nonlinear phenomena," *IEEE Trans. Microwave Theory Tech.*, Vol. 47, 2075–2084, 1999.
26. Robert, P., *Electrical and Magnetic Properties of Materials*, Artech House, 1988.